

Phase separation in the 2D Hubbard model: a fixed-node quantum Monte Carlo study

A. C. Cosentini,^{1,2} M. Capone,^{1,2,3} L. Guidoni,^{1,2,3} and G. B. Bachelet^{1,2}

¹*Istituto Nazionale di Fisica della Materia (INFM), Italy*

²*Dipartimento di Fisica, Università di Roma La Sapienza, Piazzale Aldo Moro 2, I-00185 Rome, Italy*

³*International School for Advanced Studies (SISSA-ISAS), I-34014 Trieste, Italy*

(December 2, 2024)

Fixed-node Green's function Monte Carlo calculations have been performed for very large 16×16 2D Hubbard lattices and large interaction strengths $U = 10, 20$, and 40 . For each value of U we have obtained $15 \sim 20$ densities n between empty and half filling. Up to $\sim 3/4$ filling we can safely rule out the possibility of a phase separation. Beyond $\sim 3/4$ filling, instead, this prediction seems to hold only for $U = 40$, while for $U = 10$ and 20 the prediction of a phase separation is also possible within the MC error bars. A finer mesh of data points is thus needed - and can be obtained by the same method adopted here - to safely address the issue of phase separation close to half filling. This also suggests that previous predictions based on smaller lattices and a coarser density mesh are unlikely to give reliable predictions in this density range.

PACS numbers: 71.10.Fd, 71.45.Lr, 74.20.-z

Strongly correlated electrons and holes are generally expected to play a key role in the high- T_c superconductors. Their possible instability towards phase separation (PS), initially believed to inhibit superconductivity, is attracting a lot of interest since a few different authors [1–3] have pointed out that such a tendency may in fact be intimately related to the high- T_c superconductivity. Long-range repulsive interactions may turn the PS instability into an incommensurate charge-density-wave (CDW) instability, but the very existence of a quantum critical point associated to it may be a crucial ingredient of the superconducting transition [4]. PS and/or CDW instabilities are related to a substantial reduction of the kinetic energy, which otherwise tends to stabilize uniformly distributed states; such a reduction is typical of strongly correlated electrons, both in real and model systems. PS has been experimentally observed in $\text{La}_2\text{CuO}_{4+\delta}$ [5,6], in which the oxygen ions are able to move: in the doping interval $0.01 \leq \delta \leq 0.06$ the compound separates into a nearly stoichiometric antiferromagnetic phase and a superconducting oxygen-rich phase. In generic compounds, where charged ions cannot move, the possibility of a macroscopic PS is spoiled by the long range Coulomb repulsion and should lead to an incommensurate CDW instability [7], but here the identification of charge inhomogeneities with spoiled PS is less straightforward [8]. On the theoretical side, evidence for PS has been suggested for various models of strongly correlated electrons, as the $t-J$ model [10], the three-band Hubbard model, the Hubbard-Holstein model and the Kondo model (see e.g. Ref. [4] and references therein). Despite intensive studies, even for some simple models there is no general agreement on the PS boundary: for the very popular $t-J$ model, PS is fully established only at large J , but at small J (which unfortunately happens to be the phys-

ically relevant case) theoretical and numerical results are quite controversial. Given the approximate relationship linking $t-J$ and Hubbard models [9], it is for example difficult to reconcile Emery *et al.*'s [10] theory that PS occurs at *any* value of J in the $t-J$ model, with the more recent suggestion by Gang Su [11], according to which the Hubbard model does not show PS at *any* value of U/t . Dagotto *et al.*'s [3] numerical results, suggesting no tendency toward PS for both the Hubbard model and the $t-J$ model below a critical value $J < J_c \sim t$, seem to be consistent with Gang Su's work [11] and with Shih *et al.*'s [12] recent numerical results, but are at odds with another numerical study by Hellberg and Manousakis [13]. Both theoretical and numerical results focus on thermodynamical stability, which requires the energy density \mathcal{E} of an infinite system to be a convex function of the electron density n . We can write the stability condition $\chi^{-1} = \partial^2 \mathcal{E} / \partial n^2 > 0$. PS is associated with a vanishing inverse compressibility χ^{-1} ; if χ^{-1} vanishes in a given density range $n_1 < n < n_2$, then the system is not stable and will separate into two subsystems with densities n_1 and n_2 . The available exact numerical results are however limited to very small systems (the behavior of the infinite 2D lattice must often be extrapolated from 4×4 lattices), and probably suffer from significant size effects. Under these circumstances the availability of the fixed-node Green's function Monte Carlo (FNMC), a new and powerful numerical technique [14] which allows the study of (previously unfeasible) large lattice-fermion systems, provides us with a strong motivation to further investigate the Hubbard model. Whether the 2D Hubbard hamiltonian, a prototype for interacting electrons with no long-range repulsion, shows any instability towards PS, is a very interesting open question. A numerical study may also shed some indirect light on two related issues:

the $t-J$ model in the physical region of small J , and the adequacy of the one-band Hubbard hamiltonian to catch the essential physics of real high- T_c superconductors.

To evaluate the ground-state energy of the Hubbard hamiltonian

$$H = -t \sum_{\langle i,j \rangle \sigma} (c_{i\sigma}^\dagger c_{j\sigma} + h.c.) + U \sum_i n_{i\uparrow} n_{i\downarrow} \quad (1)$$

we thus implemented the FNMC method recently proposed for lattice fermions by van Bemmel *et al.* [14,15], which has been successfully used by Boninsegni for frustrated Heisenberg systems [16] and by Gunnarsson *et al.* for orbitally-degenerate Hubbard models [17].

The Green's function Monte Carlo, after a sufficiently long imaginary time, projects out the “bosonic” (nodeless) ground-state component of any initial wavefunction; apart from transient estimates, which for large systems appear to be hazardous unless the initial variational wavefunction is sufficiently close to the exact one, this method is therefore not directly usable for fermions (and for any other system whose ground-state wavefunction has nodes). The FNMC [14,15] replaces the true hamiltonian by an effective hamiltonian which confines the Monte Carlo random walk within a single nodal region (a region of the configuration space where the guiding wavefunction never changes sign), and, in analogy with the continuum case [18,19], it provides an upper bound for the true ground-state energy [15]. Most results of this paper are based on standard MC runs of $1000 \sim 2000$ walkers, but towards the end of this work we have switched to the new and powerful Calandra-Sorella prescription for the so-called bias correction, which, as we independently checked, allows equally accurate results with just $100 \sim 200$ walkers [20].

The variational wavefunctions we use to guide the random walks and to fix the nodes are of the Gutzwiller type, being the product of a Gutzwiller factor and two Slater determinants of single-particle, mean-field wavefunctions for up- and down-spin electrons. The optimal Gutzwiller parameter and mean-field wavefunctions (whose only parameter is the staggered magnetization) are preliminarily obtained by variational Monte Carlo (VMC) runs.

A few representative variational and FNMC energies are shown in Table I for the 4×4 Hubbard lattice, for which exact results [21] are available. As expected, the VMC energy is always above the FNMC energy, which in turn is slightly above the exact energy. For comparison we show the Constrained-Path Monte Carlo (CPMC) energies of Zhang *et al.* [22], which also include a larger 16×16 lattice (last row). Especially at large U 's our results appear of comparable quality as theirs. As far as the 4×4 results are concerned, we notice that for $N_e = 10$, which corresponds to a closed-shell configuration, both FNMC and CPMC are much closer to the exact energy than for $N_e = 14$, which corresponds to an

open-shell configuration. This could be a serious problem when numerically studying the behavior of the energy as a function of the density, but our results show that for large enough lattices (see Figs. 2 and 3) these shell effects tend to disappear.

Our numerical study proceeds in two steps: first we fix the number of electrons to a constant value N_e and vary the electron density $n = N_e/N_s$ between 0 and 1 by choosing many different square or slightly rectangular Hubbard lattices, the number of sites N_s being either $L \times L$ or $L \times (L + 1)$; for each of these lattices we perform an independent VMC run followed by a FNMC run, and obtain the corresponding ground-state energy and statistical error. This amounts to the less usual way of varying the density suggested by Ref. [13] to avoid the Fermi-surface shape dependence on the number of electrons, and we want to double-check its size dependence by repeating the whole procedure for $N_e = 16, 32$ and 128 . The corresponding three sets of data for $U = 10$ are shown in Fig. 1 as full dots, diamonds and squares. The energies obtained for the smaller system ($N_e = 16$, full dots) are connected by thick black lines to emphasize their change of convexity as a function of the density, a finding which could optimistically be interpreted as a finite-size signal of the system's tendency towards PS instability in the thermodynamic limit. But when we repeat the same procedure with a higher number of electrons (and correspondingly larger lattices), the change of convexity found for the $N_e = 16$ -electron system just disappears : the diamonds (corresponding to $N_e = 32$) and the squares ($N_e = 128$) evidently fall on a nice, regular curve, whose curvature appears positive everywhere. From Fig. 1 we then conclude that the change of convexity observed at $N_e = 16$ (full dots) is an artifact of the small system, and is wiped out as the system size increases towards the thermodynamic limit. Besides their physical message, these results also seem to suggest that the less usual way of varying the density proposed by Ref. [13], which we have used up to this point, is as bad as (in fact, worse than) the more usual prescription for small systems, and as good as any other prescription for large systems: in Fig. 1 the $N_e = 32$ and 128 data are almost exactly on the thin line, which was, instead, obtained by varying the electron number N_e for a large, fixed 16×16 lattice.

These tests convinced us that for a more systematic study (more densities and more U values) we may safely stick to a large 16×16 lattice ($N_s = 256$ sites), and vary the number of electrons N_e to yield electronic densities $n = N_e/N_s$ ranging from empty $n = 0$ to half filling $n = 1$. In Fig. 2 we show the electronic ground-state energy per site, obtained by our FNMC runs as a function of the density. Antiperiodic boundary conditions are adopted [23] and energies are as usually in units of the hopping parameter t throughout this paper. The calculated points are shown as full dots for average densities corresponding to

closed shells, and as empty dots for empty shells. From Fig. 2 (and also from Fig. 3, see later) it appears that the open-shell error, which was significant for a small 4×4 lattice, see Table I, is almost negligible (i.e. of the order of our statistical error) for our large lattice [24]. The statistical errors are in turn smaller than the dot size, and thus are not visible on Fig. 2; the solid lines are three-parameter polynomial best fits of the form $-4n + an^2 + bn^3 + cn^4$. At low density, near $n=0$, the three sets of data for $U=10$ (lower), 20 (middle), and 40 (upper curve) correctly recover the expected behavior $\mathcal{E} = -4n$, also found for the noninteracting case $U=0$ (lower dashed curve in Fig. 2) and for the fully spin-polarized case (upper dashed curve). Close to half filling, near $n=1$, they also display a reasonable trend: for larger U the curves are closer, but always below, the fully spin-polarized energy (upper dashed curve); the fact that slightly above $3/4$ filling the $U=40$ curve almost touches the fully spin-polarized curve is probably due the variational nature of our FNMC energies, which always fall slightly above the exact energy (see Table I). Finally, at half filling $n=1$, the ground-state energy per site turns out to be approximately proportional to $J = 4t^2/U$ with a negative coefficient of ~ 1.13 , which compares reasonably well with the $S=1/2$ quantum Heisenberg antiferromagnet [25]. The comparison of Figs. 1 and 2 and the $U=40$ results for a smaller 12×12 lattice (shown in Fig. 2 as empty triangles), all indicate that even for medium-sized systems (smaller than our largest 16×16 lattices) all the energies nicely fall on the same curve, whose curvature appears positive all the way thru between empty and half filling.

In summary, the results presented so far suggest that within the MC statistical error our 16×16 FNMC energies for the $2D$ Hubbard model do not depend on different ways of varying the density, on open-shell effects, and on size effects. For all U 's considered here a naive polynomial fit predicts a positive curvature everywhere, which would amount to the absence of PS. A more careful analysis of our data is thus needed to double-check such a prediction [26]. The large density ($n \sim 1$) region is expected to be the one in which PS, if present, should occur. In our polynomial fits all data points are treated on the same footing, and this can lead to an underestimate of PS effects. An alternative path to the study of PS is the standard Maxwell's construction. It has been shown in Ref. [10] that this procedure is completely equivalent to study, as a function of the hole density $x = 1 - n$, the quantity $e(x) = [e_h(x) - e_H]/x$, i.e., the energy per hole measured relative to e_H , the energy for $x=0$ [in our previous symbols $e_h(x) = \mathcal{E}(n=1-x)$]. For a sufficiently large system, if the energy per site $\mathcal{E}(n)$ depends linearly on the electronic density n between some critical density n_c and half filling (the fingerprint of PS which we seem to miss in the polynomial fits of Fig. 2), then for $x < x_c$ (i.e., above a given density $n_c = 1 - x_c$) the function $e(x)$

is constant (independent of x). Therefore the fingerprint of a PS is here a range of x values where the plot of $e(x)$ is horizontal. The presence or absence of powers higher than 1 in the expansion of $\mathcal{E}(n)$ near $n=1$ translates into the difference between a nonzero and a zero slope of $e(x)$ near $x=0$, which should be appreciated much better than the difference between a straight line and a small portion of a parabola in Fig. 2. In some sense, $e(x)$ works like a magnifying lens of our PS. It should be stressed that in a consistent definition of $e(x)$ the half-filling energy e_H must be obtained as $e_h(x=0)$ from the *same* calculation as the other $e_h(x \neq 0)$ values (in this work, from our FNMC). If that's not the case, as sometimes found in the literature [13], then $e(x)$ will inevitably tend to diverge near $x=0$: in general towards plus infinity, since the variational energies are always above the exact value, in which case we'll always find a minimum somewhere between $x=0$ and $x=1$. In other words, an inconsistent definition of $e(x)$ can artificially create, rather than magnifying, the occurrence of PS. Fig. 3 presents a plot of $e(x)$ based on the same datasets shown in Fig. 2. In the upper left panel we see the three $e(x)$ datasets corresponding to the three $\mathcal{E}(n)$ datasets of Fig. 2. The solid lines reproduce the fits of Fig. 2. The upper data are $U=10$, the middle are $U=20$, and the lower $U=40$. We see that for $U=10$ and 20 our polynomial best fits (which, as said, have a positive curvature all the way thru in the $\mathcal{E}(n)$ plot) perfectly follow the FNMC results almost everywhere, except very close to $x=0$, where the last two-three calculated points seem to depart from them. The error bars on $e(x)$ are obtained from the original FNMC error bars (invisible on Fig. 2) as the sum of the statistical errors on the calculated $e_h(x \neq 0)$ and $e_H = e_h(x=0)$ divided by x . Because of these denominators, they start to become visible below $x \simeq 0.5$ in Fig. 3, and become larger and larger as x approaches zero.

Perhaps the most suggestive case is $U=20$ (magnified in the lower left panel of Fig. 3). Here the last calculated FNMC points close to $x=0$ present a minimum around $x \simeq 0.1$. For $U=10$ (upper right panel), where we have less points near $x=0$, the FNMC results are more ambiguous; they could suggest either a zero or a positive slope of $e(x)$ as $x \rightarrow 0$. Therefore our data points, which clearly indicate the absence of PS for $x > 0.25$, cannot definitively rule out the possibility of PS for smaller hole densities. Finally for $U=40$ (lower right panel, where also the 12×12 points are shown as triangles), the slope of $e(x)$ is definitely positive for any calculated small value of x . Even if it is expected that the critical value x_c moves closer to $x=0$ as U is increased, our data points do not indicate any tendency towards a zero slope for all the calculated points between $x=0.06$ and $x=1$.

However, even in the suggestive case of $U=20$, we cannot draw a clear-cut conclusion: once they are translated into the $e(x)$ plots, our data acquire, as mentioned, large error bars (see Fig. 3 and caption). In other words, the

magnifying lens also magnifies the error bars; a non-zero and a zero slope are both within the error bars in Fig. 3, just like, in Fig. 2, a straight and curved line could be both compatible with our last 2-3 points near $n=1$, if we had omitted the rest of the data points. If this is the state of the art with our large lattices, then the results of previous numerical simulations, based on smaller lattices, should probably be taken with great caution as an evidence either in favor or against PS.

As far as our results are concerned, we therefore conclude that, for the coupling values considered here, the Hubbard model does not show PS below 3/4 filling, but, at lower hole densities, more energies and/or smaller error bars are required for any prediction to be really safe. These numerical investigations are underway.

We thank M. Boninsegni, S. Sorella, O. Gunnarsson, and M. Grilli for useful suggestions and a critical reading of this manuscript, C. Castellani for an illuminating discussion, and A. Filippetti for his precious help. Special thanks are due to V.J. Emery and S.A. Kivelson, whose remarks were of key importance for the final discussion of our results, and to M. Calandra and S. Sorella for making available to us the method of Ref. [20] prior to publication. GBB gratefully acknowledges partial support from the Italian National Research Council (CNR, Comitato Scienza e Tecnologia dell'Informazione, grants no. 96.02045.CT12 and 97.05081.CT12), the Italian Ministry for University, Research and Technology (MURST grant no. 9702265437) and INFM Commissione Calcolo.

[1] M. Grilli, R. Raimondi, C. Castellani, C. Di Castro, and G. Kotliar, Phys. Rev. Lett. **67**, 259 (1991); C. Di Castro and M. Grilli Physica Scripta T **45**, 81 (1992), and reference therein.
[2] V.J. Emery, and S.A. Kivelson, Physica C **209**, 597 (1993).
[3] E. Dagotto, A. Moreo, F. Ortolani, D. Poilblanc and J. Riera, Phys. Rev. B **45**, 10741 (1992).
[4] C. Castellani, C. Di Castro, M. Grilli, Phys. Rev. Lett. **75**, 4560 (1995).
[5] J.D. Jorgensen, B. Dabrowski, Shiyon Pei, D.G. Hinks, L. Soderholm, B. Morosin, J.E. Schirber, E.L. Venturini, and D.S. Ginley, Phys. Rev. B **38**, 11337 (1988).
[6] F.C. Chou *et al.*, Phys. Rev. B **54**, 572 (1996).
[7] J.M. Tranquada, B.J. Sternleb, J.D. Axe, Y. Nakamura, and S. Uchida, Nature **375**, 561 (1995).
[8] A. Bianconi, N.L. Saini, A. Lanzara, M. Missori, T. Rossetti, H. Oyanagi, H. Yamaguchi, K. Oka, and T. Ito, Phys. Rev. Lett. **76**, 3412 (1996).
[9] The $t-J$ model at small J (with $J=4t^2/U$) does not exactly reproduce the Hubbard model in the large- U limit, but the difference between the models is much more relevant on spectral properties than on their ground-state energies (the relevant quantity for PS).
[10] V.J. Emery, S.A. Kivelson, H.Q. Lin, Phys. Rev. Lett. **64**, 475 (1990).
[11] Gang Su, Phys. Rev. B **54**, R8281 (1996).
[12] C.T. Shih, Y.C. Chen and T.K. Lee, cond-mat/9705156.
[13] C.S. Hellberg and E. Manousakis, Phys. Rev. Lett. **78**, 4609 (1997).
[14] H.J.M. van Bemmel, D.F.B. ten Haaf, W. van Saarloos, J.M.J. van Leeuwen, G. An, Phys. Rev. Lett. **72**, 1442 (1994).
[15] D.F.B. ten Haaf, H.J.M. van Bemmel, J.M.J. van Leeuwen, W. van Saarloos, and D.M. Ceperley, Phys. Rev. B **51**, 13039 (1995).
[16] M. Boninsegni, Phys. Rev. B **52**, 15304 (1995); Phys. Lett. A **216**, 313 (1996).
[17] O. Gunnarsson, E. Koch, and R.M. Martin, Phys. Rev. B **54**, R11026 (1996); *ibid.* **56**, 1146 (1997); F. Aryasetiawan, O. Gunnarsson, E. Koch, and R.M. Martin, Phys. Rev. B **55**, 10165 (1997).
[18] J.B. Anderson, J. Chem. Phys. **63**, 1499 (1975).
[19] D.M. Ceperley, Physica B **108**, 875 (1981).
[20] M. Calandra and S. Sorella, Phys. Rev. B, in print.
[21] A. Parola, S. Sorella, S. Baroni, R. Car, M. Parrinello, and E. Tosatti, Physica C **162-164**, 771 (1989); A. Parola, S. Sorella, M. Parrinello, and E. Tosatti, Phys. Rev. B **43**, 6190 (1991).
[22] Shiwei Zhang, J. Carlson, and J.E. Gubernatis, Phys. Rev. Lett. **74**, 3652 (1995).
[23] Different boundary conditions yield energies within an error bar for 16×16 lattices and within at most two error bars for our smallest lattices; all results presented here refer to antiperiodic boundary conditions.
[24] The density dependence of the systematic FNMC error of the 4×4 lattice seems to be mostly related to open-shell effects, which we found to be negligible for lattices larger than 12×12 .
[25] Q.F. Zhong and S. Sorella, Euro. Lett. **21**, 629 (1993).
[26] V.J. Emery, and S.A. Kivelson, private communication (1998).

size	N_e	n	U	VMC	FNMC	CPMC	EXACT
4×4	10	0.625	4	-1.211(2)	-1.220(2)	-1.2238(6)	-1.2238
4×4	10	0.625	8	-1.066(2)	-1.086(2)	-1.0925(7)	-1.0944
4×4	14	0.875	8	-0.681(2)	-0.720(2)	-0.728(3)	-0.742
4×4	14	0.875	12	-0.546(2)	-0.603(2)	-0.606(5)	-0.628
16×16	202	0.789	4	-1.096(2)	-1.107(5)	-1.1193(3)	-

TABLE I. Ground-state energy per site (in units of the hopping parameter t) for a 4×4 Hubbard lattice and various values of U . N_e is the number of electrons and n is the corresponding average density. VMC: variational Monte Carlo, this work; FNMC: Fixed-Node Green's function Monte Carlo, this work; CPMC: Constrained-Path Monte Carlo, Ref. [21]; EXACT: exact diagonalization results, Ref. [20].(see text)

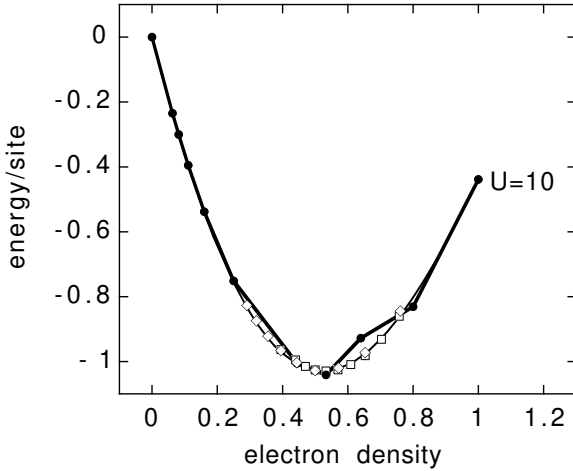


FIG. 1. Ground-state energy per site (in units of the hopping parameter t) as a function of the electronic density, for finite 2D Hubbard lattices at $U=10$. The electronic density is varied by keeping the number of electrons N_e constant and varying the size of the lattice. Full dots and thick solid line: $N_e=16$; diamonds: $N_e=32$; squares: $N_e=128$. The polynomial best fit of the $U=10$ data of Fig. 2 (see text) is shown for comparison as a thin solid line.

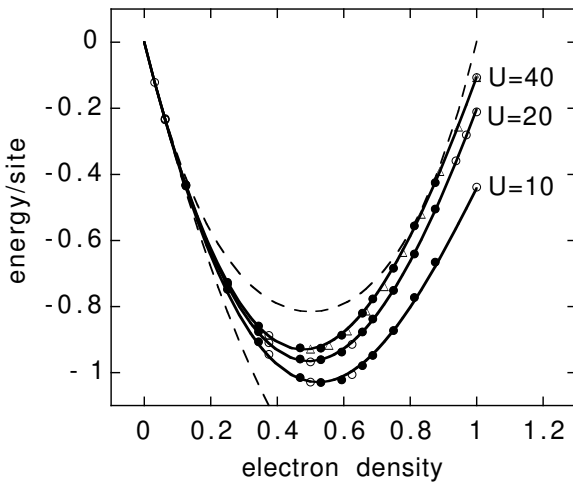


FIG. 2. Ground-state energy per site (in units of the hopping parameter t) as a function of the electronic density, for a 2D Hubbard lattice of $N_s = 16 \times 16 = 256$ sites with $U = 10$ (lower), 20 (middle), and 40 (upper data). The electronic density varies from 0 to 1 as the number of electrons N_e is varied from 16 to 256. Errors are smaller than the dot size. Full dots correspond to closed shells and empty dots correspond to empty shells. The solid curves which connect calculated points are three-parameter polynomial fits (see text). The dashed curves represent, instead, known analytical results: the upper one is the fully spin-polarized energy, which is symmetric with respect to quarter filling; the lower one is the $U = 0$ noninteracting energy. The empty triangles, obtained for a smaller 12×12 lattice and $U = 40$, are shown for comparison (see text).

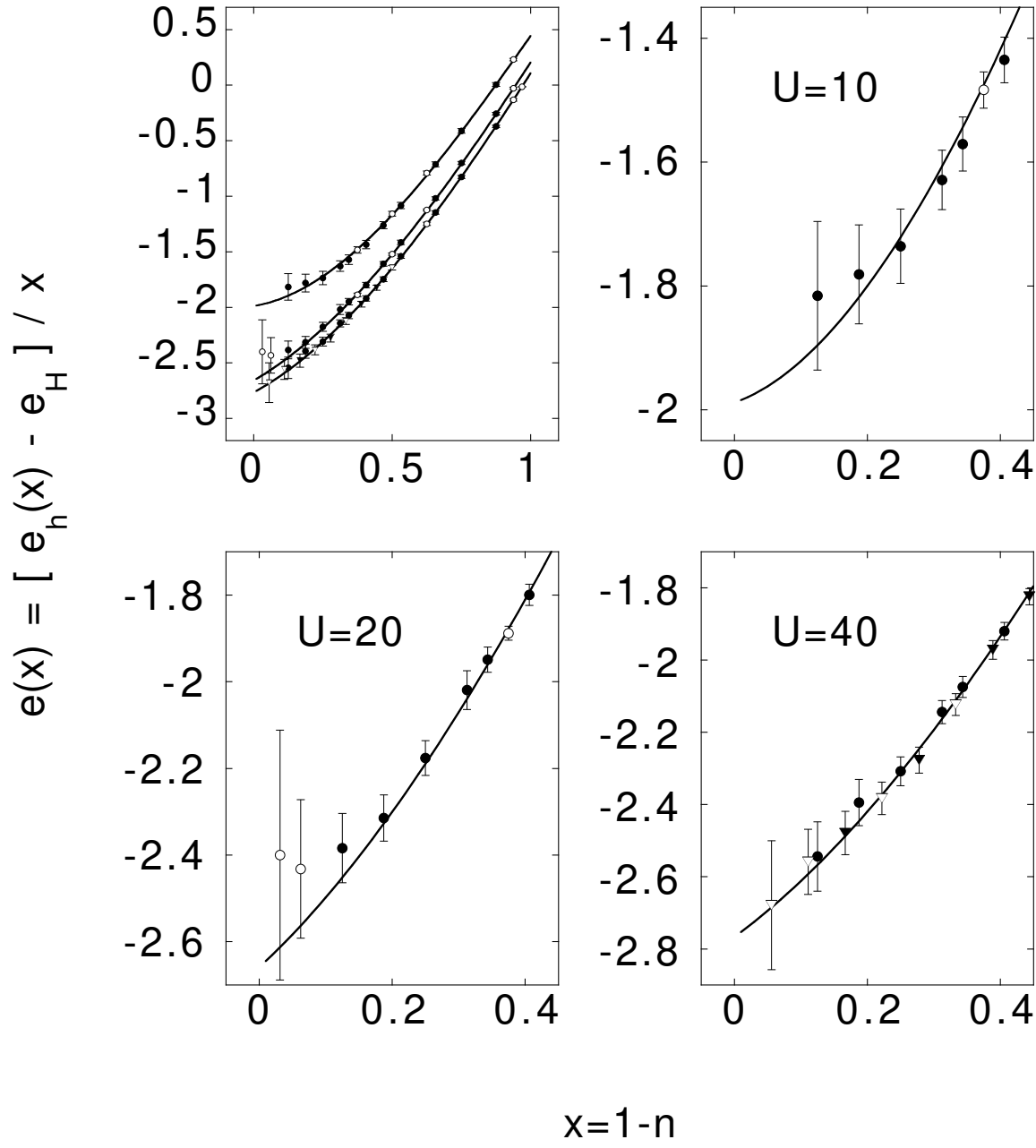


FIG. 3. Plot of $e(x)$ vs. x (see text) for a 2D Hubbard lattice of $N_s = 16 \times 16 = 256$ sites with $U = 10$ (upper), 20 (middle), and 40 (lower data). x varies from 0 to 1 as the number of electrons N_e is varied from 256 to 0. Full dots correspond to closed shells and empty dots correspond to empty shells. The solid curves reproduce the three-parameter polynomial fits of the previous figure. The triangles (empty for empty shells and full for closed shells), obtained for a smaller 12×12 lattice and $U = 40$, are shown for comparison. The error bar associated to each $e(x)$ is obtained as $\Delta e(x) = [\Delta e_h(x) + \Delta e_h(x=0)]/x$ where $\Delta e_h(x)$ is the statistical FNMC error (see text).